

Enhanced PVDF Properties by Multi-Wall Carbon Nanotubes (MWCNT) for Efficient Energy Harvesting

Jie Hu and Tzuyang Yu
Department of Civil and Environmental Engineering
University of Massachusetts Lowell
One University Avenue, Lowell, MA 01854, U.S.A.

ABSTRACT

Piezoelectric materials such as polyvinylidene fluoride (PVDF) or lead zirconate titanate (PZT) are the fundamental materials for fabricating piezoelectric based energy harvesters. However, the drawbacks for these two materials are: (i) poor mechanical properties of PZT (e.g., brittle, low fracture stress); (ii) low energy efficiency of PVDF. Extensive research work has been made on investigating the piezoelectric property of PVDF. But very few attentions have been paid on mechanical property. In this paper, we report a synthesization of PVDF using a very low multi-wall carbon nanotubes (MWCNT) fraction in PVDF to enhance both the mechanical property and piezoelectricity of PVDF/MWCNT composite. Through a series of well-controlled experiments, we found that the adding of MWCNT in PVDF affects the crystalline structure. Our experimental result also showed that the maximum tensile stress and maximum piezoelectric voltage constant both occurs at PVDF/MWCNT (0.05wt%). With the the MWCNT fraction exceeded 0.05wt%, the maximum tensile stress and maximum piezoelectric voltage constant decreased.

Keywords: Polyvinylidene fluoride (PVDF), multi-wall carbon nanotubes (MWCNT), piezoelectricity, mechanical property

1. INTRODUCTION

Energy harvesting (also known as energy scavenging) is the process of capturing the ambient waste energy (e.g., solar energy, kinetic energy, etc.) and converting it into electricity. This harvested electricity can be used to power small electronic devices, such as wireless sensors or wearable electronics. Among all those energy harvesting technologies, piezoelectric energy harvesting is one of the most popular one. In reported piezoelectric energy harvester systems, materials such as polyvinylidene fluoride (PVDF) or lead zirconate titanate (PZT), have been widely used. Roundy proposed a two-layer bending element. In their experiments, a piezoelectric generator was fabricated from a two-layer PZT-5A. Under a vibration source of 2.5 ms^{-2} at 120 Hz, their harvester generated a power output of $375 \mu\text{W}$ with 1 cm^3 in size.¹ A PZT-Stack energy harvester was reported by Xu. Through a series of well-controlled experiments, they found that 35% of mechanical energy can be converted into electricity. And their energy conversion efficiency is 4 times more than others.² A heel strike electric generator was presented by Howells. This generator was made of four PZT-5A bimorph stacks. Extracted, stored and regulated by the heel strike system, the output voltage of this system was 12 VDC.³ Reilly reported a trapezoidal piezoelectric harvester, which was focused on a resonant frequency and strain concentration. With a given acceleration and resonant frequency, the harvested energy was used to power a radio for a duty cycle of 0.2%.⁴ However, the poor mechanical property of PZT (e.g., brittle, low fracture stress) and low energy efficiency of PVDF limit their applications in powering high energy consuming devices or high stress condition.

To overcome these limitations, extensive research work has been conducted in the past few years. When mixing an appropriate amount of carbon nanotubes in PZT/PVDF, the piezoelectric performance of the composite could be improved.⁵ A two-step process for synthesizing PVDF/reduced graphene oxide (PVDF/rGO) was developed by Huang. They found that the β phase concentration in PVDF/rGO composite improved greatly than pure PVDF with 0.1 wt% rGO. The experiment results also showed that the piezoelectric charge constant

Further author information: (Send correspondence to T. Yu)
E-mail: tzuyang-yu@UML.EDU, Telephone: 1 978 934 2288

of the composite increased by 78.6%.⁶ A PZT/Nylon57 composite was produced by Supmak et al in 2008. The composite was found to have a maximum piezoelectric charge constant of 28 pC/N. The relative permittivity was 73 and the remnant polarization was around 138 $\mu\text{C}/\text{cm}^2$.⁷ A PZT-Zn ionomer composite was reported by James. Compared with PZT-polymer composite, such as PZT-ethylene methacrylic acid copolymer (EMAA), PZT-Zn possessed excellent fatigue performance even at strain level of 4% and high piezoelectric charge constant.⁸ Even if these pilot studies have made some achievements, the potential of synthesized PVDF with MWCNT composite has not been fully understood. The goal of this study is to develop an energy efficient PVDF/MWCNT composite.

The objective of this paper is to investigate the effect of different MWCNT fraction on PVDF/MWCNT composites, followed by the method of synthesizing the composites. Mechanical property, Attenuated total reflection-Fourier transform infrared (ATR FT-IR) spectrum and piezoelectricity of the composites are characterized. Experimental results are discussed and findings are summarized.

2. THEORETICAL BACKGROUND

Pure PVDF and its composites have a crystalline structure, which is consist of four typies of phase (α, β, γ and δ phase).⁹ γ and δ phase are not commonly investigated. α phase is formed due to the polymer crystallization from melt state. For β phase, it is formed from the polymer chain distortion and planar zigzag.¹⁰ Among those phases, only β phase has an influence on piezoelectricity of polymer. There are two forms of piezoelectricity: direct and inverse. For direct piezoelectricity, electrical charges are generated by dielectric materials due to the existing mechanical stress, as defined by Eq. (1):

$$D = \varepsilon^\sigma E + d\sigma \quad (1)$$

where D = electrical displacement, ε^σ = the dielectric permittivity as at a constant stress field, E = electrical field, and d and σ = piezoelectric charge constant and mechanical stress, respectively. The stress and electrical fields are both considered in Eq. (1). However, this is not reality due to the low generated electrical field (E). Therefore, the $\varepsilon^\sigma E$ in Eq. (1) can be ignored and the equation becomes:

$$D = d\sigma \quad (2)$$

For inverse piezoelectricity, strain is obtained when piezoelectric materials are subjected to an electric field. The relationship between strain and piezoelectric charge constant is described in Eq. (3):

$$\delta = S\sigma + dE \quad (3)$$

where S = mechanical compliance of material. Similarly, Eq. (3) can be simplified as:

$$\delta = dE \quad (4)$$

Piezoelectric effects can also be evaluated by the piezoelectric voltage constant. Compared with the piezoelectric charge constant, the piezoelectric voltage constant is focused on voltage generated by the material. Eq. (5) presents the relationship of those two parameters.

$$d = K^T \varepsilon_0 g \quad (5)$$

where K^T = linked to capacitance of poling electrodes, ε_0 = dielectric permittivity in vacuum and g = the piezoelectric voltage constant.

3. EXPERIMENTION

In our experiment work, the first step was to synthesize PVDF/MWCNT composite at different MWCNT fraction levels. Mechanical property of PVDF/MWCNT composites was then measured, followed by the investigation of ATR FT-IR spectrum. The composites were further polarized under 100 V and 70°C. The piezoelectricity of the PVDF/MWCNT composites was studied at last.

3.1 PVDF/MWCNT Preparation

The matrix PVDF particles were supplied by a commercial vendor (Sigma Aldrich), whose Weight Average Molecular Weight (Mw) was 455,000 and Number Average Molecular Weight was 110,000. The MWCNT was also purchased from the same vendor. The purity of the MWCNT was 98% and its average length was 6-13nm \times 2.5 – 20 μ m. The Dimethylformamide (DMF) solvent was supplied by Sigma Aldrich. Its density and boiling temperature were 0.944 g/cm³ and 152°C, respectively.

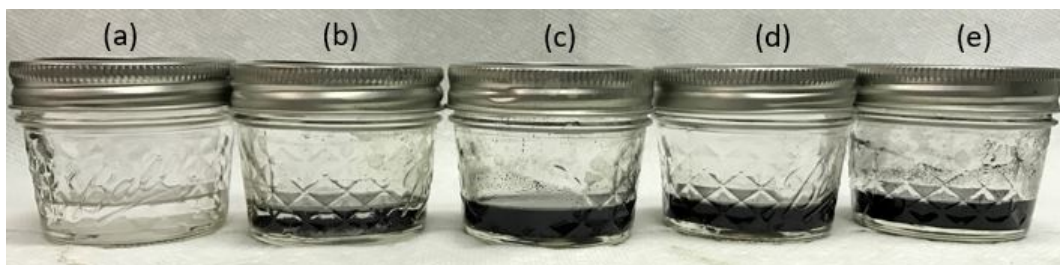


Figure 1. PVDF/MWCNT solution; (a) 0wt%; (b) 0.05wt%; (c) 0.1wt%; (d) 0.5wt%; (e) 1wt%.

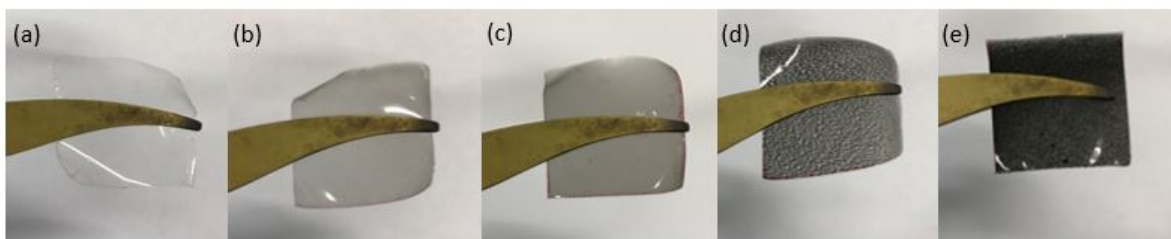


Figure 2. PVDF/MWCNT composites: (a) 0wt%; (b) 0.05wt%; (c) 0.1wt%; (d) 0.5wt%; (e) 1wt%.

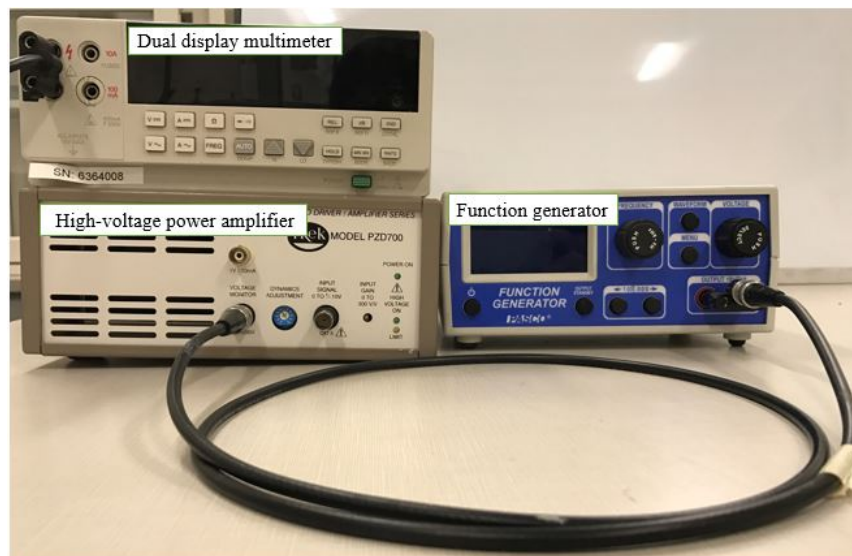


Figure 3. Function generator, power amplifier and multimeter.

MWCNT with five different fractions (0wt%, 0.05wt%, 0.1wt%, 0.5wt%, 1wt%) was dissolved in a DMF solvent. To enhance the dispersion performance of MWCNT in DMF, a sonicator (PH750EL, Iultrasonic) and a hot plate (Corning Hot Plate/Stirrers, Carolina) was used. The MWCNT/DMF solution was ultrasonically processed for 1.5 hours. After MWCNT was fully dissolved, PVDF particles were added into the black solution.

This mixture was heated and stirred on a hot plate for another 12 hours. The heating temperature and stirring speed were set as 50°C and 500 rpm, respectively. Figure 1 shows the mixed PVDF/MWCNT solution. To produce homogeneous PVDF films, the PVDF/MWCNT solution mixture was poured on a rectangular glass (10 cm × 10 cm), which was fixed on the chamber of a spin coater (WS-650, Laurell). The rotation speed of the spin coater was 150 rpm and duration time was 40 s. The obtained PVDF membranes were evaporated in room temperature for 24 hours to form PVDF/MWCNT composites. Figure 2 depicts the produced composites.

3.2 Mechanical Property Measurement

Mechanical property of the PVDF/MWCNT composites was performed by an universal material testing system (Instron Model 4400). PVDF/MWCNT composites were cut into 40 mm × 10 mm and clamped between two clips of the instrument in a tensile test configuration. The strain rate of the machine was set as 10 mm/min. Up to five samples were tested in each MWCNT fraction group.

3.3 FT-IR Spectrum

To develop the ATR FT-IR spectrum, NICOLET 670 was used. The composites were cut into 5 mm × 5 mm. Because FT-IR is very sensitive to impurities, the composites need to be carefully cleaned before measurement. The FT-IR spectrum of PVDF/MWCNT was obtained and the results were recorded.

3.4 Polarization

Piezoelectric performance of PVDF/MWCNT is poor before polarization. Therefore, to improve its piezoelectricity, poling the composites is required. PVDF/MWCNT composites were cut into 20 mm × 20 mm and covered with copper (used as the electrode). According to previous research work, the polarization quality was subjected to poling temperature, time and voltage.¹⁰ In this experiment, the poling voltage we used was 100 V and the poling temperature was 70°C. This high voltage was achieved by function generator (PASCO®), high-voltage power amplifier (TREK MODEL PZD700) and dual display multimeter (FLUKE 45), which were shown in Figure 3. To heat the PVDF/MWCNT composites uniformly and protect it from breaking down in high voltage and in air, silicon oil (XIAMETER® PMX-200) bath was utilized. The oil was heated to the 70°C and the composites were submerged into it during polarization. Up to three samples were polarized and the duration was 30 min . The setup of the polarization was given in Figure 4.

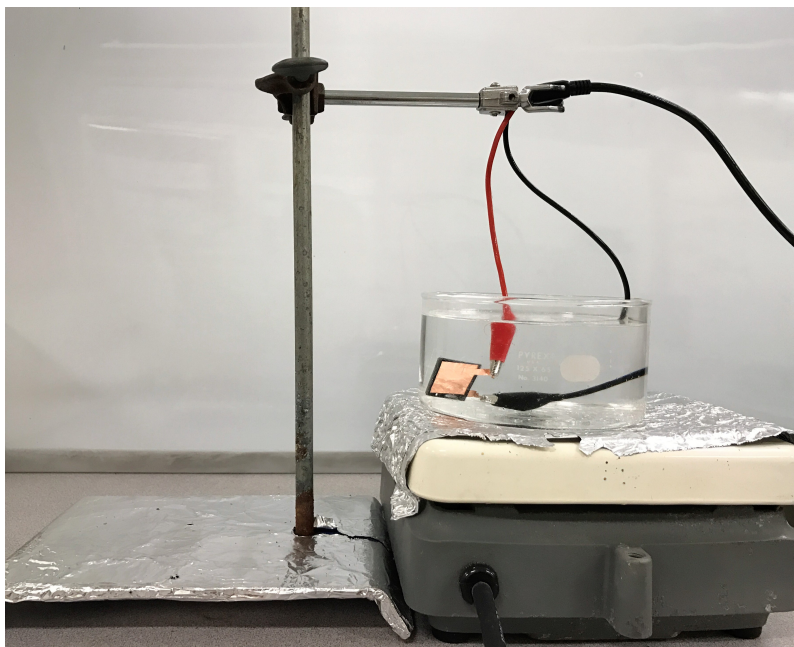


Figure 4. Polarization setup.

3.5 Piezoelectric Measurement

To investigate the piezoelectricity of the composite, Fluke multimeter (Fluke 289 TRUE RMS) was utilized. The PVDF/MWCNT composites were fixed on a testing table and two electrodes were connected to the multimeter. 1.32 N static force was applied on the sample and the generated voltage was recorded. Up to three samples were tested in each MWCNT fraction group. The piezoelectricity measurement setup was illustrated in Figure 5.

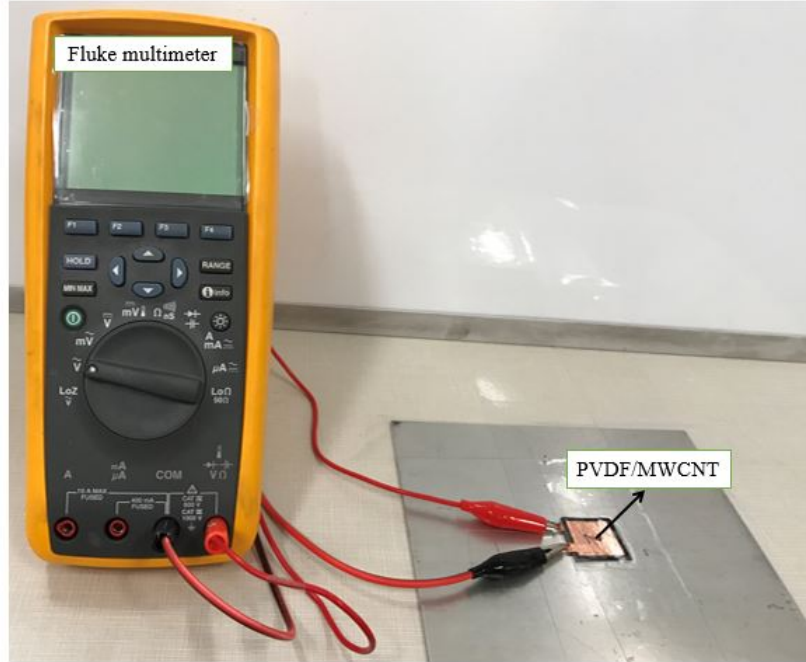


Figure 5. Piezoelectric measurement setup.

4. RESULTS AND FINDINGS

In this paper, we investigated three properties of PVDF/MWCNT composites: mechanical, chemical and piezoelectric properties. The main results and findings are discussed in the following.

4.1 Mechanical Property

The tensile strain vs. tensile stress curve of the PVDF/MWCNT composites was shown in Figure 6. It was observed that the mechanical property of the composites varies with the MWCNT fraction. Compared with ductility of PVDF/MWCNT composites at different MWCNT fraction levels, it was found that the maximum ductility occur in pure PVDF. When increasing the fraction from 0% to 0.05wt%, the ductility reduced from 897.9% to 585.2%. However, when keeping increasing the MWCNT fraction from 0.05wt% to 1wt%, the ductility of the composites decreased significantly. The maximum tensile stress was found when the MWCNT fraction is 0.05wt%. The maximum tensile stress decreased when the MWCNT fraction increase from 0.05wt% to 1wt%. Based on Figure 6, the curve of maximum tensile strain of PVDF/MWCNT composites at different MWCNT fraction levels was illustrated in Figure 7. It was found that increasing MWCNT fraction is detrimental to the maximum tensile strain of PVDF/MWCNT composites. It was also observed that the maximum tensile strain decrease sharply when MWCNT fraction is between 0wt% and 0.1wt%. However, after the MWCNT fraction went beyond 0.1wt%, the maximum tensile strain reduced in a relatively slow rate. To better understand the relationship between the maximum tensile strain and MWCNT fraction, a model was proposed.

$$\epsilon_{max} = \frac{46.91}{\omega + 0.0505} \quad (6)$$

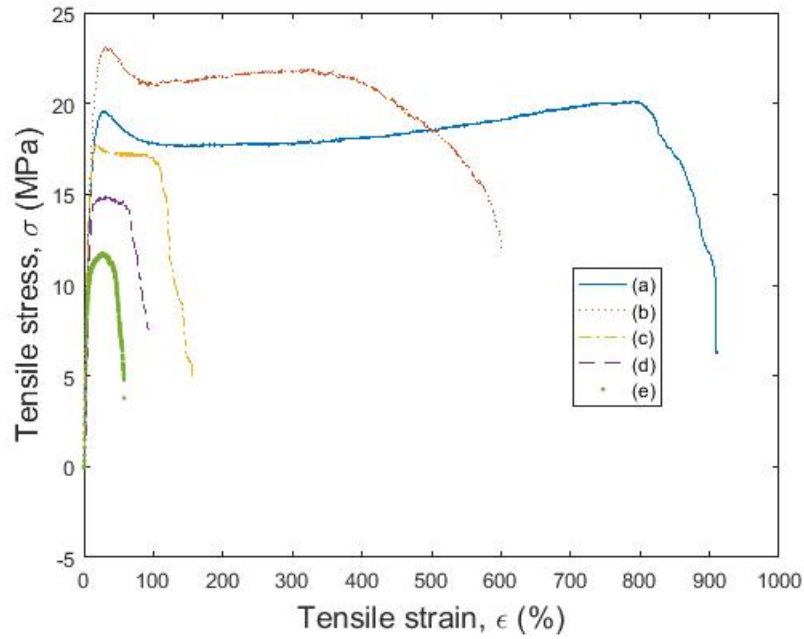


Figure 6. Tensile stress vs tensile strain of PVDF/MWCNT ocomposites with different MWCNT fraction level: (a) PVDF; (b) PVDF/MWCNT (0.05wt%); (c) PVDF/MWCNT (0.1wt%); (d) PVDF/MWCNT (0.5wt%); (e) PVDF/MWCNT (1wt%).

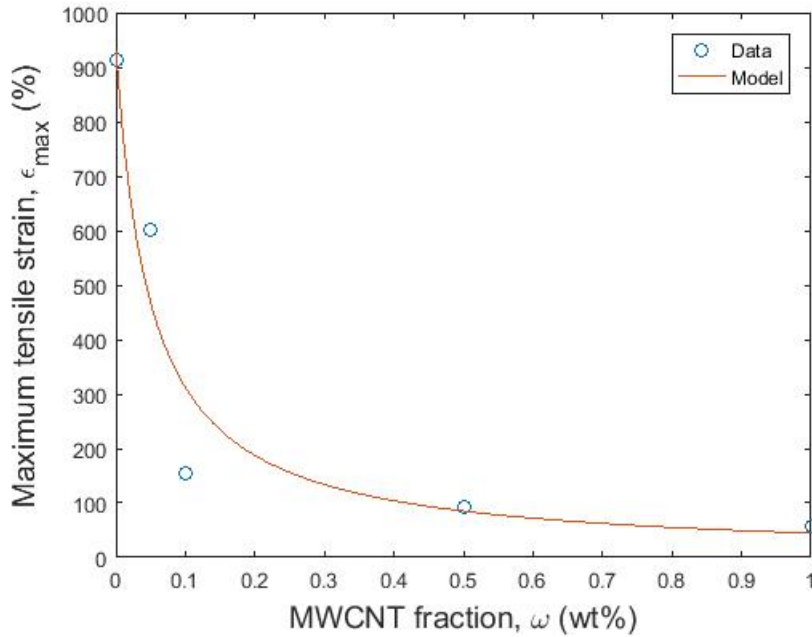


Figure 7. Maximum tensile strain vs MWCNT fraction.

where ϵ_{max} = maximum tensile strain (%) and ω = MWCNT fraction (wt%). The enlarged section of Figure 6 in the MWCNT fraction range of $\epsilon=0-0.048\%$ was Figure 8. It was found that the initial tensile stress is approximately linear with tensile strain. Figure 8 also denoted that initial tensile stress and tensile strain curve fluctuated with the MWCNT fraction. When linear regression was applied to each curve in Figure 8, Young's

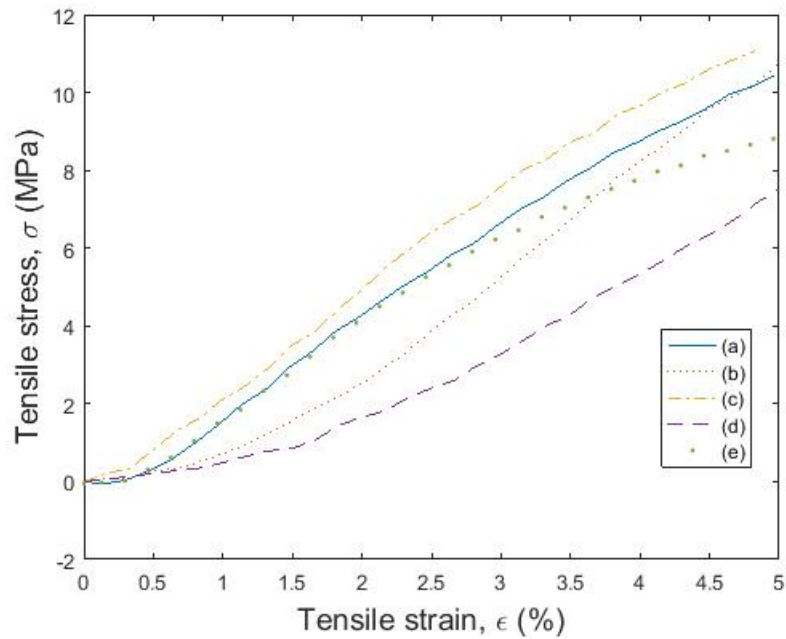


Figure 8. Zoomed in tensile stress and tensile strain curve of PVDF/MWCNT composites with different MWCNT fraction level:(a) PVDF; (b) PVDF/MWCNT (0.05wt%); (c) PVDF/MWCNT (0.1wt%); (d) PVDF/MWCNT (0.5wt%); (e) PVDF/MWCNT (1wt%).

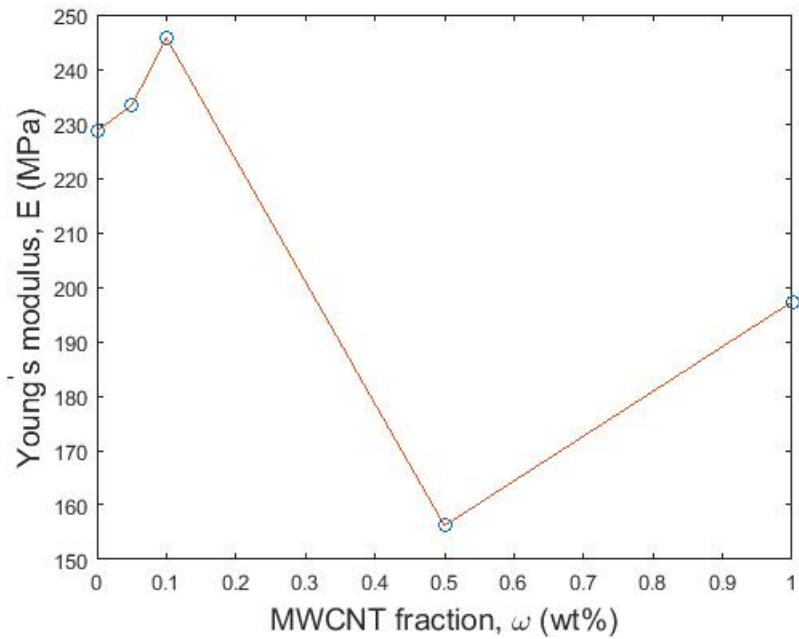


Figure 9. Young's modulus vs MWCNT fraction.

modulus of the PVDF/MWCNT composites were obtained, which was shown in figure 9. The maximum Young's modulus occurred when MWCNT fraction was 0.1wt%, whereas the minimum Young's modulus was found in 0.5wt%. It was observed that the Young's modulus fluctuated with the MWCNT fraction. According to Figure 6, the correlation between MWCNT fraction and maximum tensile stress was obtained, which was given in Figure

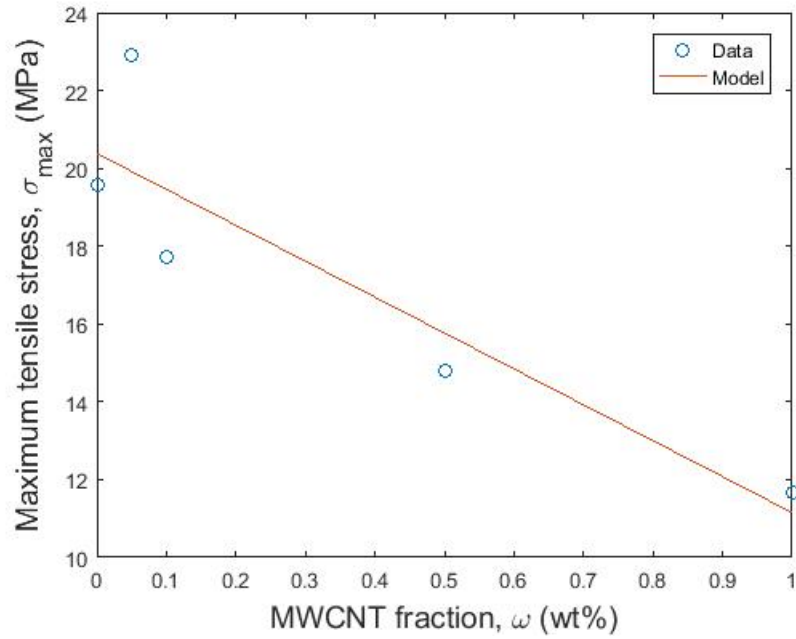


Figure 10. Maximum tensile stress vs MWCNT fraction.

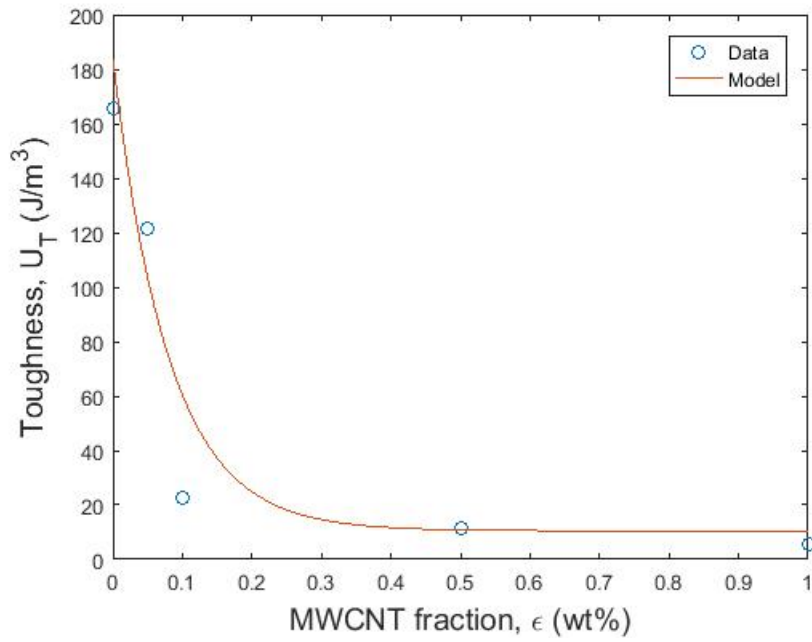


Figure 11. Toughness vs MWCNT fraction.

10. The maximum tensile stress σ_{max} at various MWCNT fraction levels was modeled as:

$$\sigma_{max} = 9.226\omega + 20.38 \quad (7)$$

where σ_{max} = maximum tensile stress (MPa) and ω = MWCNT fraction (wt%). Figure 10 indicated that the maximum tensile stress of PVDF/MWCNT composite decreases when the MWCNT fraction increases. More specifically, when the MWCNT fraction was higher than 0.05wt%, the maximum tensile stress went down.

According to the Figure 10, the highest maximum tensile stress occurs at 0.05wt% of MWCNT fraction. However, this does not mean that the highest maximum tensile stress occurs exactly at 0.05wt%. To accurately determine the optimal MWCNT fraction that produces the highest tensile stress, additional experiments such as a smaller MWCNT fraction are required. Compared with Figures 10 and 7, it is interesting to learn that there is a tradeoff between the maximum tensile stress and maximum tensile strain, suggesting that the maximum tensile strain does not appear in the same MWCNT fraction as the maximum tensile does. The toughness of the PVDF/MWCNT composites at different MWCNT fraction was illustrated in Figure 11. The maximum toughness was observed in pure PVDF. When increasing the MWCNT fraction, the toughness of the composites decrease. And this reduction becomes sharply between 0 and 0.1wt% MWCNT fraction range. When the MWCNT fraction exceeded 0.1wt%, relatively less reduction of the toughness was observed. The toughness and MWCNT fraction was modeled as following:

$$U_T = 172.9e^{-12.45\omega} + 10.5 \quad (8)$$

where U_T = toughness (J/m^3) and ω = MWCNT fraction (wt%).

4.2 Chemical Property

The ATR FT-IR spectrums of pure PVDF and PVDF/MWCNT composites were given in Figure 12. The peaks of α phase was found in 610 cm^{-1} and 760 cm^{-1} in each curve, which were attributed to skeletal bending and CF_2 bending, respectively. When compared with each MWCNT fraction group, the strongest α phase peak was found in pure PVDF, whereas the weakest α phase peak was found in 1wt%. When increasing the MWCNT fraction, the α phase peak decreased gradually. However, the peaks of β phase appeared in 810 cm^{-1} (CH_2 rocking) and 1140 cm^{-1} (CF_2 stretching). With the increasing MWCNT fraction from 0 to 1wt%, the peaks of β phase was increased. This phenomenon indicated that the addition of MWCNT in PVDF contribute to the formation of β phase.

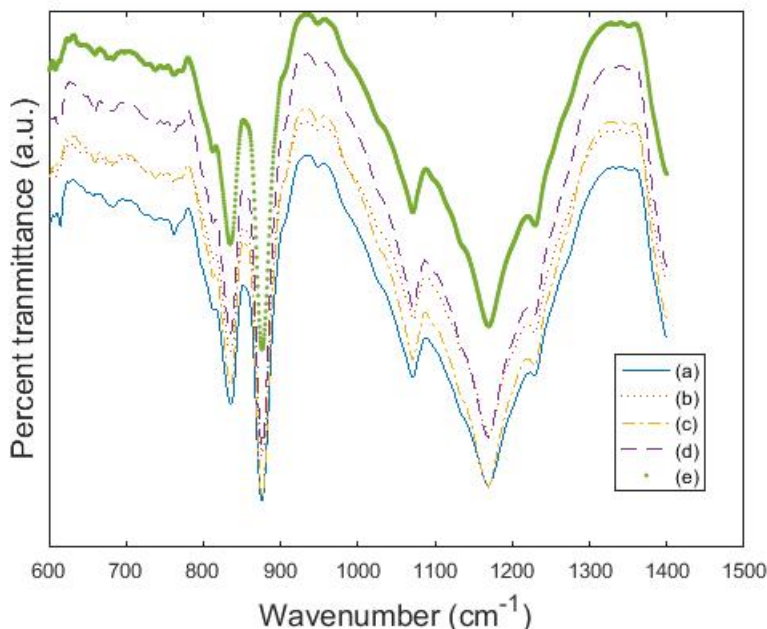


Figure 12. FT-IR spectrum of PVDF/ MWCNT composites with different MWCNT fraction level: (a) PVDF; (b) PVDF/MWCNT (0.05wt%); (c) PVDF/MWCNT (0.1wt%); (d) PVDF/MWCNT (0.5wt%); (e) PVDF/MWCNT (1wt%).

4.3 Piezoelectric Property

The piezoelectric voltage constants of PVDF/MWCNT composites with different MWCNT fraction were displayed in Figure 13. It demonstrated that piezoelectric voltage constant varies with the MWCNT fraction. When increasing MWCNT fraction, the piezoelectric voltage constant slightly increased at first (0.05wt%) and decreased when the MWCNT fraction exceeded 0.05wt%, which meant higher MWCNT fractions are detrimental to piezoelectricity of PVDF/MWCNT composites. The maximum piezoelectric voltage constant was obtained when MWCNT fraction was the 0.05wt%. However, when comparing the piezoelectric voltage constant of pure PVDF with PVDF/MWCNT (0.05wt%), the improvement of piezoelectric voltage constant was approximately 7.4%. Based on Figure 13, the piezoelectric voltage constant and MWCNT content was modeled as:

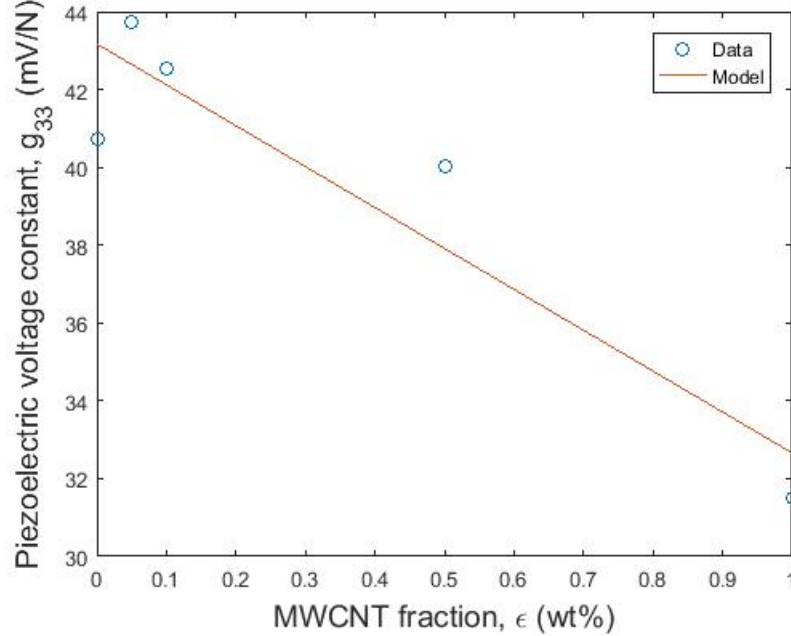


Figure 13. Piezoelectric voltage constant with MWCNT fraction.

$$g_{33} = 0.51\omega + 43.17 \quad (9)$$

where g_{33} = piezoelectric voltage constant (mV/N) and ω = MWCNT fraction (wt%).

5. CONCLUSION

In this paper, the procedure of synthesizing PVDF/MWCNT composites and material characterization (mechanical, chemical and piezoelectric property) is reported. It is found that the maximum tensile stress occurs when the MWCNT fraction is 0.05wt%. The maximum tensile stress decreases when the MWCNT fraction increase from 0.05wt% to 1wt%. The maximum ductility and the maximum tensile strain are both observed in pure PVDF. The initial tensile stress and tensile strain curve fluctuates with MWCNT fraction. The maximum Young's modulus is found when MWCNT fraction was 0.1wt%, whereas the minimum Young's modulus is found in 0.5wt%. It is observed that the peaks of β phase appears in 810 cm^{-1} and 1140 cm^{-1} . With the increasing MWCNT fraction from 0 to 1wt%, the peaks of β phase is increased. The piezoelectric voltage constant slightly increases at first (0.05wt%) and decreases when the MWCNT fraction exceeded 0.05wt%. The maximum piezoelectric voltage constant is obtained when MWCNT fraction is the 0.05wt%. This work demonstrates the PVDF/MWCNT is a prospective material for energy harvesting.

6. ACKNOWLEDGMENT

This work was partially supported by the University of Massachusetts Lowell. In addition, Dr. Min Wang from Department of Chemistry of UMass Lowell and Dr. Christopher Niezrecki from Department of Mechanical Engineering of UMass Lowell were greatly acknowledged.

REFERENCES

- [1] Roundy, S. and Wright, P. K., "A piezoelectric vibration based generator for wireless electronics," *Smart Materials and structures* 13(5), 1131 (2004).
- [2] Xu, T.-B., Siochi, E. J., Kang, J. H., Zuo, L., Zhou, W., Tang, X., and Jiang, X., "Energy harvesting using a pzt ceramic multilayer stack," *Smart Materials and Structures* 22(6), 065015 (2013).
- [3] Howells, C. A., "Piezoelectric energy harvesting," *Energy Conversion and Management* 50(7), 1847–1850 (2009).
- [4] Reilly, E. K., Burghardt, F., Fain, R., and Wright, P., "Powering a wireless sensor node with a vibration-driven piezoelectric energy harvester," *Smart Materials and Structures* 20(12), 125006 (2011).
- [5] Guan, X., Zhang, Y., Li, H., and Ou, J., "Pzt/pvdf composites doped with carbon nanotubes," *Sensors and Actuators A: Physical* 194, 228–231 (2013).
- [6] Huang, L., Lu, C., Wang, F., and Wang, L., "Preparation of pvdf/graphene ferroelectric composite films by in situ reduction with hydrobromic acids and their properties," *RSC Advances* 4(85), 45220–45229 (2014).
- [7] SUPMAK, W., PETCHSUK, A., and THANABOONSOMBUT, A., "Influence of ceramic particle sizes on electrical properties of lead zirconate titanate (pzt)/nylon57 composites," *Journal of Metals, Materials and Minerals* 18(147-151) (2008).
- [8] James, N., Lafont, U., Van der Zwaag, S., and Groen, W., "Piezoelectric and mechanical properties of fatigue resistant, self-healing pzt-ionomer composites," *Smart Materials and Structures* 23(5), 055001 (2014).
- [9] Hu, J. and Tao, J., "Energy harvesting from pavement via pvdf: Hybrid piezo-pyroelectric effects," in [Geo-Chicago 2016], 556–566.
- [10] Dargaville, T. R., Celina, M. C., Elliott, J. M., Chaplya, P. M., Jones, G. D., Mowery, D. M., Assink, R. A., Clough, R. L., and Martin, J. W., "Characterization, performance and optimization of pvdf as a piezoelectric film for advanced space mirror concepts," Sandia Report SAND2005-6846. Sandia National Laboratories (2005).